ELSEVIER

International Journal of Mass Spectrometry 181 (1998) 43–50

International Journal of Mass Spectrometry

Application of laser induced photoemission electron in time-of-flight mass spectrometry

Li Wang, Haiyang Li, Jiling Bai*, Xiaoqing Hua, Richang Lu

State Key Laboratory of Molecular Reaction Dynamics, Dalian Institute of Chemical Physics, Chinese Academy of Science, Dalian 116023, P.R. China

Received 8 May 1998; accepted 14 August 1998

Abstract

Multicharged ions of Ar and NO were observed in multiphoton ionization (MPI) experiments while a focused laser beam struck extractor grid of time-of-flight mass spectrometry (TOF-MS). A special photoemission electron impact ionizer was designed. This ionizer made it possible to investigate the mechanism of photoelectron impact ionization. The experiment showed that the multicharged ions could be produced only by the photoelectron impact, probably ionized step by step. With this special ionizer high Rydberg states ($n \sim 40 - 100$) of atoms and/or molecules were, for the first time, observed in the TOF-MS. The yield ratio of Rydberg states to ions was strongly dependent of the laser power and the energy of the photoemission electrons. Our experiment results showed that this ionizer could be an effective method for producing multicharged ions and high Rydberg states of atoms and molecules. (Int J Mass Spectrom 181 (1998) 43–50) © 1998 Elsevier Science B.V.

Keywords: Photoemission electron; Multicharged ions; High Rydberg states

1. Introduction

Time-of-flight mass spectrometer (TOF-MS) has been finding an increasingly wide variety of applications. The mass resolution of TOF-MS is mainly determined by the temporal and spatial distribution of ions [1]. Because of this, multiphoton ionization (MPI) [2] has been widely used in the ionization of TOF-MS. By the use of a tunable, ultrashort pulsed laser, resonance enhanced multiphoton ionization (REMPI) has been applied to TOF-MS, that made the mass spectrum with high selectivity and high mass resolution. On the other hand, the high selectivity is not suitable to the analysis of unknown species. The narrow band of the laser light can only ionize those species that absorb the photons with specific frequencies. It is well known that electron impact ionization (EI) is a versatile method to ionize all kinds of molecules, which has been widely used in conventional mass spectrometers [3]. The key problem in the use of EI to TOF-MS is how to generate a short pulsed electron beam with high intensity. There were a few reports [3–5] in which a conventional electron gun was used in TOF-MS. With these electron guns, the sensitivity and mass resolution [4,5] of the mass spectrometers were not comparative to that with MPI traditional electron gun in TOF-MS.

* Corresponding author; E-mail: jlbai@rose.dicp.ac.cn

PII S1387-3806(98)14159-3

Laser induced photoelectron emission from metal surfaces has been widely studied and applied to TOF-MS since the 1980s [6–16]. The short pulsed electron beam made it possible to improve the mass resolution in TOF-MS with EI. Subsequently, multi-charged ions [13–16] were observed. These reports showed that the laser induced photoemission electron impact ionization could be a good complement to the MPI in TOF-MS for analysis of unknown species.

In this paper, we present our observations in our TOF-MS experiments with laser induced photoemission electron impact ionization. A special ionizer was designed to control the intensity and energy of the photoemission electrons by changing laser power and electron accelerating voltage, respectively. Interestingly, high Rydberg (HR) states of atoms and molecules were also observed in our experiments [17]. The ions could be separated from neutral Rydberg species in the spectra by an initially pre-setting small dc electric field, which was quite similar to the process of mass analysis threshold ionization (MATI) [18].

2. Experimental setup

The experiments were carried out with our home-made linear TOF-MS [19]. Briefly, the TOF-MS consisted of two chambers: a molecular beam source chamber and an ionization flight chamber. The sample gas, injected through a pulsed valve (General Valve 900, 0.5 mm nozzle diameter), was skimmed before entering the ionization region. Ions produced in this ionization region were then extracted and accelerated into a field free region, detected by a three-stage microchannel plate detector (MCP), and recorded by a 100 MHz digital transient recorder. With the molecular beam on, pressures of source chamber and ionization-flight chamber were maintained lower than 10^{-3} and 10^{-4} Pa, respectively. A detailed description of the experiment controlling and the data acquisition system had been described elsewhere [20]. The molecular beam, laser beam and the ion flight axis were perpendicular to each other.

In the typical configuration as shown in Fig 1(a), a focused laser beam was directed onto the extractor

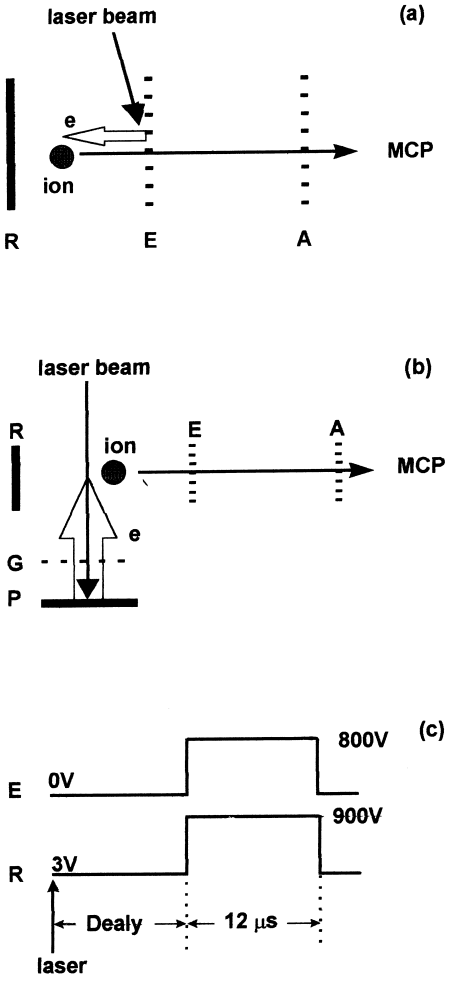

Fig. 1. Configurations of the TOF-MS ionizer: (a) typical ionizer, (b) modified ionizer, and (c) voltages for MATI setup.

grid (E) where the photoelectrons were produced. Both the photoelectrons and the ions produced in the ionizer could be accelerated by either a dc high voltage or pulsed high voltage (900 V with 200 ns of rising edge and 12 μs of duration) across the repeller (R) and accelerator (A) (stainless steel meshes with 85% of optical transmission). The accelerator grid was always connected to the ground.

In order to control the photoelectron independently, that is to separate the ion acceleration from acceleration of the photoelectrons and the electron impact ionization process, a special modification has been made in the ionizer configuration, as shown in

Fig 1(b). A stainless steel plate (P), with negative potential (VE), was placed on the laser path as a target for generating photoelectrons. A copper mesh (G) was placed 10 mm over the target plate and connected to the ground. The laser beam was well aligned without striking either the repeller plate or the extractor grid. The energy of the photoelectrons generated from the target could be adjusted by changing the potential of the target plate.

In the course of electron impact, atoms and molecules can be either ionized into ions, or excited up to neutral electronically excited states (Rydberg states), or both occur [20]. In order to separate the ions from the neutral states of molecules, a small offset voltage was preset across the repeller and extractor grid of the TOF-MS as shown in Fig 1(c). The offset voltage was kept at 3 V/cm in our experiments. Under this condition, the ions, produced by direct EI, started moving towards the extractor at the moment they were produced, while the moving of the neutral species during the short delay time (several microseconds) was almost negligible. These high Rydberg species could be ionized by field ionization when the delayed HV pulsed electric field came (100 V/cm between the repeller plate and extractor grid) and started to move to the detector, resulting in longer arrival time than the ions. In the TOF mass spectra, the arrival time of the neutral species was maintained with almost no change with the time delay, while the arrival time of the ions varied with the delay time of the HV pulse.

3. Experimental results

3.1. With conventional ionizer

With the conventional ionizer in TOF-MS as shown in Fig. 1(a), XeCl excimer laser (Lambda-Physic EMG-50, 308 nm, 10 ns) was used in the following experiments. The laser beam was slightly focused by an $f = 400$ mm lens and directed onto the extractor grid.

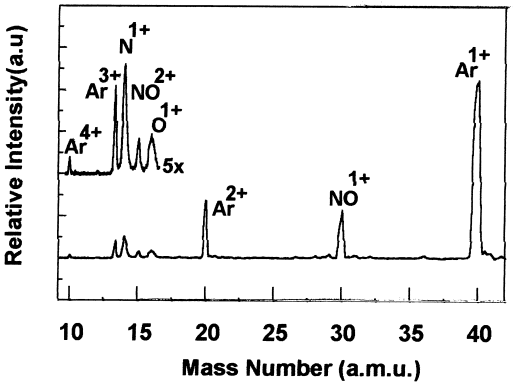

Fig. 2. Mass spectrum of 10% NO in Ar.

3.1.1. Observations of the multicharged ions

With 10% NO mixed in Ar used as a sample gas, a typical mass spectrum was presented in Fig. 2.

As expected, the NO^{1+} and Ar^{1+} ions were observed. It was interesting that the ions NO^{2+} and multicharged Ar up to +4 charged states also appeared.

It is known that the ionization potential (IP) of Ar^{3+} to Ar^{4+} is 59.8 eV [21] and the appearance potential (AP) of Ar^{4+} ion is 144.1 eV, which means that an Ar atom should have absorbed more than 30 photons of 308 nm (4.0 eV) at the same time if it was ionized through MPI. This was impossible with the laser power in our experiment condition ($<10^6$ W/cm^2). The other evidence was that no ion was found, even NO^{1+}, when the laser beam passed through the ionization region without striking either the repeller plate or the extractor grid. This implied that the sample gas was ionized by the laser induced photoelectrons from the grid surface.

3.1.2. Effect of delayed HV pulsed acceleration field

To clarify the ionization mechanism further, the constant dc voltage across the acceleration field was switched to the delayable pulsed high voltage. The delay time between the laser pulse and the rising edge of the high voltage pulse could be adjusted from 0 to a few microseconds.

The result obtained with this regime is shown in Fig. 3. With the delay time of zero, the mass spectrum

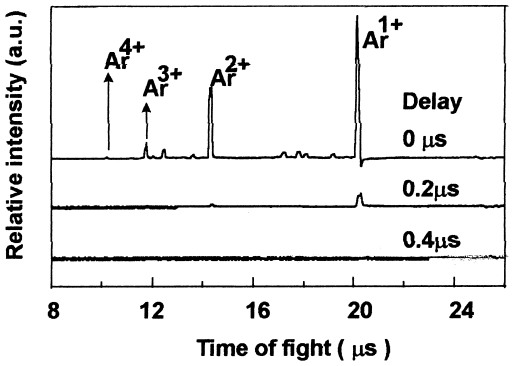

Fig. 3. TOF mass spectra of Ar vs delay time.

was similar to that obtained with the dc acceleration field. The significant difference was that no ion could be seen when the delay time was longer than 0.2 μs. This implied that the MPI or laser desorption ionization (LDI) could be ruled out. If the ions were produced by MPI or LDI, they should have survived in the ionizer for several microseconds and have been detected, because not all the ions could have moved out of the space of the ionizer (10 mm $\times$ 10 mm) with the thermal velocity (about 0.5 mm/μs) in a few microseconds.

Considering the low energy and high velocity of the photoelectrons, the results in Fig. 3 are understandable. The photoelectrons were unable to ionize the gas atoms until they gained enough energy in the HV electric field. Because the mass of electron is very small, its velocity is very fast even at low energy level (about 600 mm/μs with 1 eV kinetic energy). When the HV acceleration field built up a bit later, the photoemitted electrons could move out of the ionizer without ionizing any species in the ionization region. Consequently no ions could be detected. This is important evidence for the ionization mechanism of the photoemission electron impact.

3.2. With the new design of the ionizer (the modified ionizer)

With the modified ionizer, the energy of the photoemission electrons could be independently controlled. A primary investigation of the effect of the impact energy of the photoelectrons on the ionization process had been carried out.

The second harmonic output 532 nm of Nd:YAG laser (Spectra-Physics GCR 170) with pulse duration of 8 ns was used in these experiments. The laser beam was slightly focused by a f = 820 mm lens and directed onto the stainless steel target as shown in Fig. 1(b). The laser beam was carefully aligned that neither the repeller nor the extractor was struck on. The diameter of the circular light spot on the target plate was about 3 mm. The photoelectrons emitted from the target were then accelerated in the electric field between the copper mesh and the target plate. The energy of the photoelectrons was roughly determined by the voltage on the target plate (VE). The ions, produced by electron impact, were extracted, then accelerated by the delayed high voltage pulse.

3.2.1. Formation of multicharged ions

The TOF mass spectrum of argon gas obtained with the modified regime is shown in Fig. 4, where VE was kept at -200 V, and the delay time of the HV pulse was 1 μs. Comparing to Fig. 3, the difference is obvious. The argon ions as well as multicharged ions could be observed even at the delay time of HV pulse as long as 1 μs; while the ions almost disappeared only after about 0.2 μs. As mentioned above, the thermal velocity of the ions at room temperature is about 0.5 mm/μs without electric field. The consequence was that the ions produced by the electron

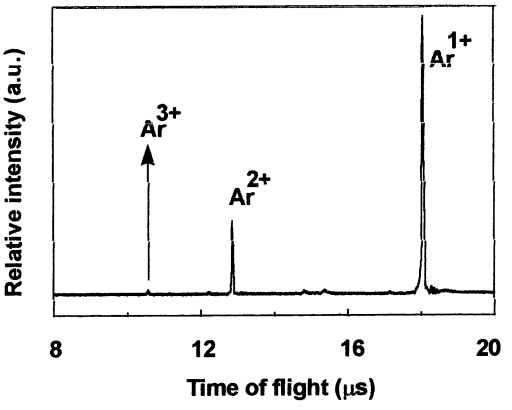

Fig. 4. TOF mass spectrum of Ar by modified ionizer.

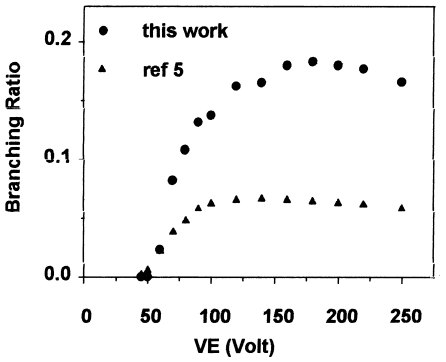

Fig. 5. Branching ratio of Ar^{2+}/Ar^{1+} vs VE.

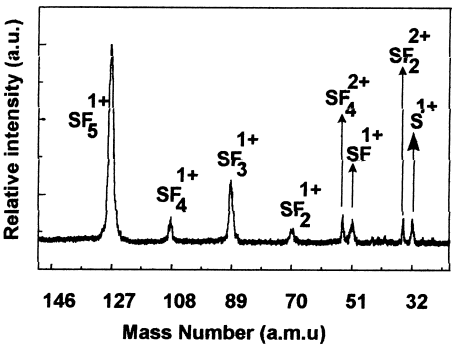

Fig. 6. Mass spectrum of SF_6.

impact could not drift out of the ionizer space and could be detected after a few microseconds delay. The reason for this was that in the modified ionizer, the photoelectron energy and ionization of the Ar atoms were not dependent on the HV of the ionizer.

3.2.2. Branching ratio of Ar^{2+}/Ar^{1+} varied with VE

Fig. 5 shows the variation of the branching ratio of Ar^{2+}/Ar^{1+} with VE. The delay time was 1 μs. The branching ratio of Ar^{2+}/Ar^{1+} increased with VE in the low VE region, approaching a constant value when VE was higher than 100 V. As a comparison, the results from [5] are also shown in Fig. 5 and were obtained by using a conventional hot filament electron gun. It is obvious that the branching ratio of Ar^{2+}/Ar^{1+} in our experiments was much greater than those obtained [5]. A possible reason for this may be the difference in the intensities of the electron beams between the two electron guns.

3.2.3. Fragmentation of polyatomic molecule SF_6

MPI of SF_6 has been studied for decades. In the present experiment, SF_6 was taken as an example of polyatomic molecules to be investigated on the fragmentation and ionization by the photoemission electron impact. As shown in Fig. 6, there were various fragment ions produced by the EI. Double charged ions of fragments SF_{2n} ($n = 1,2$) were found in the spectrum, which has never been reported in the literature with conventional mass spectrometers. This is currently being studied.

3.3. Generation of high Rydberg states

With the modified ionizer, plus an ion shifting electric field, the neutral species could be separated from the charged species in the ionizer. The Rydberg states of atoms and/or molecules, for the first time, were observed in the TOF-MS, and investigated as well.

3.3.1. Formation of high Rydberg states

The Rydberg state of argon atoms formed by photoemission electron impact was the first observed in our TOF-MS experiment. With the laser power at 5.5 mJ/pulse and VE at −16.6 V, and changing the delay time, two groups of peaks were observed in the TOF mass spectrum as shown in Fig. 7. The separation between the two groups increased with increasing the delay time. The peaks shifted by the 3 V electric field with time delay were the signals of the argon

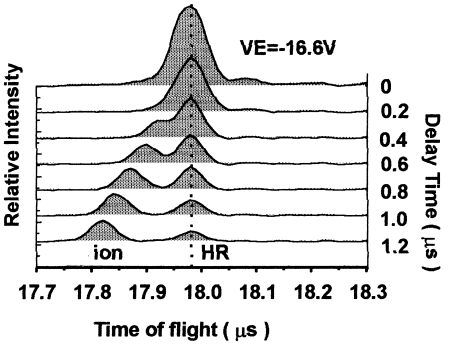

Fig. 7. TOF mass spectra of Ar ions and HR states.

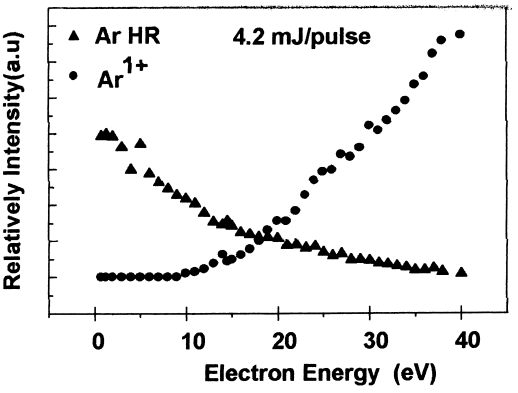

Fig. 8. Intensities of ions and HR varied with VE.

ions, and the peaks remained constant at constant arrival time must be electronically excited neutral species ionized by the HV electric field. These electronically excited neutral species were assigned as Rydberg states.

According to the formula [22,23],

$$n \approx 134/E^{1/4} \quad \text{and} \quad \delta_l/n^3 \approx 3n^2E$$

where n is the main quantum number, E is the field intensity and δ_l is the quantum defect, respectively. The observable high Rydberg states should be in the range of n from 40–100, with the quantum defect δ_l estimated from -0.5 to 0.5, under our experimental conditions.

The signal intensity of Ar ions was almost unchanged in the short time of delay, whereas the relative intensity of the Rydberg states decreased with the time delay. This decay showed further that the neutral species were in electronically high excited states. Although we could not individually isolate these Rydberg states in our current experiment, what we could get from the decay picture in Fig. 7 was the average lifetime of these Rydberg states. It was approximately several microseconds, consistent with the results of Freund et al. [24].

3.3.2. Branching ratio of Rydberg states to Ar^+

The interesting observation was that the yield ratio of high Rydberg states to Ar^+ ions was strongly dependent on VE as shown in Fig. 8. It was obvious that the ionization potential of Ar is about 15.8 eV (I.P.). When VE was lower than the ionization potential of Ar, only Rydberg states could be seen. The lower the VE, the higher the yield of Rydberg states. With VE increasing, the yield of ions went up while the Rydberg states were reduced. We were also surprised that some doubly excited high Rydberg states of Ar were also observed (not shown in this article).

3.3.3. High Rydberg states of C_2H_2 and its fragments

The ionization and fragmentation of many polyatomic molecules were studied with the modified ionizer. Fig. 9 shows one of the examples, the TOF mass spectra of C_2H_2. The laser power was about 3 mJ/pulse and VE was kept at -23 V. The ions and Rydberg states of the fragments and their parent molecules are clearly separated in the spectra. The Rydberg states of both parent molecules and their fragments obtained in the same mass spectrum provided a direct experimental evidence for the "core ion model," suggested by Freund [22]. In this model, a high Rydberg state of molecules might dissociate into two fragments, one in a high Rydberg state and the other in a ground state. To the best of our knowledge, this was the first observation of the high Rydberg states of molecules and their fragments in the same mass spectrum.

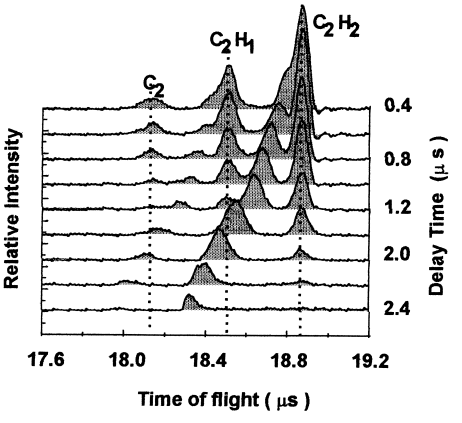

Fig. 9. TOF mass spectra of fragment ions and HR states of C_2H_2.

4. Discussion on the ionization mechanism

The FWHM of the Ar^{1+} peak in Fig. 2 was about 50–60 ns. Considering the fact that the mass resolution within these experiments was the same as that in the MPI experiments, and the broadening effect during the flight, the EI ionization process should occur in a similar short time scale as the MPI process. This means that the pulse width of the electron emission was in the same order of magnitude as the laser pulse. Because of the short width of the electron pulse, the instant intensity of the electron beam induced by pulsed laser is high.

In our experiments, the modified ionizer made it possible to separate the ionization process from the electron generation process. Because the photoelectron acceleration could be independently controlled, and the ion acceleration field was in a delayed pulse HV field, it was possible to distinguish the species ionized by MPI or EI. Under our experiment conditions, the ions were produced by laser induced photoemission electron impact ionization, the MPI mechanism could be ruled out completely.

The formation mechanism of multicharged ions is still not clear so far. We did find the multicharged ions of Ar and NO in the mass spectra under the EV lower than their appearance potentials. One possible explanation is that the ionization was proceeded step by step, that is, a multielectron impact ionization. The instant high intensity of the photoelectrons emission seems to support this consideration, but it was unlikely because the electron beam was not focused in our experiments. The other possible explanation is that the electron energy distribution was very broad because of the space charge effect. A large number of electrons might have higher energy than the nominal value of VE. The electrons with energy in excess of the appearance potential of the multicharged ions would be responsible for the formation of the multicharged ions.

There were a few articles [7–11] that reported on the photoemission generation when laser beams struck metal surfaces. When the photon energy was lower than the work function of the metal surface, multiphoton processes [10,11] were involved. The duration of the photoemission electron pulse was strongly dependent on the width and the energy of laser pulse. The intensity of the photoelectron beam could be three orders of magnitude higher than that of current conventional filament emission [11]. The major difficulty in the generation of a good electron beam is that the space charge effect cannot be easily eliminated. It could broaden the pulse duration as well as the energy distribution of the electron beam; in particular, if we want to achieve an electron beam with low energy. As we have seen above, the low energy electrons are important for the formation of Rydberg states.

The observation of the high Rydberg states was one of the most interesting discoveries in our experiments. The dependence of the yield ratio of the Rydberg states to ions upon the VE provided the possibility that we could selectively generate Rydberg states with this technique. It should, however, be noted that VE was not equal to the electron energy. Because of the effect of space charge, and the possible photoemission electrons from the copper mesh over the laser target plate, the energy distribution of the photoelectrons may be very broad. The effect of the low energy electrons on the impact process could be very different from that of high energy electrons. It is important to narrow the energy distribution of the photoelectrons for the future investigation.

There is a big argument on the formation mechanism of the high Rydberg states in the electron impact process. As shown in Fig. 7, the low VE was in favor of forming Rydberg states, whereas the low electron energy was not able to excite the atom up to such a high Rydberg state. How was the kinetic energy of the electrons transferred into the electronically excited states of the atoms or molecules? Just one step of electron impact? Or did it go through many steps, such as collision of atoms with electrons one after another, or ionized first, then recombined with an electron, forming a high Rydberg state, and so on. This article reports the results of our primary studies. Because the energy distribution was unknown, we could not tell much more about the formation mechanism at present. Because of much interest in this topic, study of the formation mechanism and dynamic characteristics of the Rydberg states is being continued in our lab.

5. Summary

In summary, a new design of a laser induced electron beam source and its application to TOF mass spectrometers were presented in this article. With this modification, a series of experiments has been carried out and the main results are summarized as follows: (1) Laser induced photoemission electron impact ionization could be applied to conventional TOF-MS as a useful complement for analysis of unknown species without any selective limitation. (2) Application of the new designed ionizer, combined with delayed high voltage pulse, has made it possible to distinguish the photoelectron impact ionization from MPI in TOF-MS. (3) The multicharged ions of Ar, NO and some other polyatomic species were produced in our TOF-MS. The formation mechanism of these ions was probed to be photoelectron impact ionization. (4) The formation of high Rydberg states of atoms, molecules, and their fragments was observed. The yield branching ratio of Rydberg states to ions was dependent of the electron impact energy. Lower impact energy was in favor of formation of Rydberg states. Doubly excited high Rydberg states of some gas atoms were also observed. Further study of the formation mechanism of the high Rydberg states and the multicharged ions by this new technique is underway.

Acknowledgements

This work was supported by the National Natural Science Foundation of China. The authors thank Dr. Jinchun Xie for helpful discussions.

References

[1] W.C. Wiley, I.H. Mclaren, Rev. Sci. Instrum. 26 (1955) 1150.
[2] Laser and Mass Spectrometry, D.M. Lubman (Ed), Oxford University Press, New York, 1990.
[3] T.D. Mark, in Gaseous Ion Chemistry and Spectroscopy, J.H. Futrell (Ed.), Wiley, New York, 1986, Chap. 3.
[4] S.T. Fountain, D.M. Lubman, Anal. Chem. 65 (1993) 1257.
[5] J.A. Syage, Phys. Rev. A 43 (1992) 5666.
[6] Y. Kawamura, K. Toyoda, M. Kawai, Appl. Phys. Lett. 45 (1984) 307.
[7] D. Charrlambidis, E. Hontzopoulos, C. Fotakis, Gy. Farkas, Cs. Toth, J. Appl. Phys. 65 (1989) 2843.
[8] Y. Kawamura, K. Toyoda, M. Kawai, J. Appl. Phys. 71 (1992) 2507.
[9] M. Aeschlimann, E. Hull, J. Cao, C.A. Schmuttenmaer, L.G. Jahn, Y. Gao, H.E. Elsayeo-Ali, D.A. Manteli, M.R. Scheinfein, Rev. Sci. Instrum. 66 (1995) 1000.
[10] M. Aeschlimann, C.A. Schmuttenmaer, H.E. Elsayed-Ali, R.J.D. Miller, J. Chem. Phys. 102 (1995) 8606.
[11] T. Tanable, Y. Kawamura, D. Li, K. Toyoda, Rev. Sci. Instrum. 66 (1995) 1010.
[12] E.R. Rohwer, R.C. Beavis, C. Kostner, J. Lindner, J. Grrotemeyer, E.W. Schlag, Z. Naturforsch. Teil A 43 (1988) 1151.
[13] J.G. Boyle, L.D. Pfefferle, E.E. Gulcicek, S.D. Colson, Rev. Sci. Instrum. 62 (1991) 323.
[14] P.Y. Cheng, H.L. Dai, Rev. Sci. Instrum. 64 (1993) 2211.
[15] S.M. Colby, J.P. Reilly, Int. J. Mass Spectrom. Ion Processes 131 (1994) 125.
[16] D.C. Schriemer, Liang Li, Rev. Sci. Instrum 66 (1995) 55.
[17] L. Wang, H. Li, J. Bai, R. Lu, Chem. Phys. Lett. 282 (1998) 204.
[18] L. Zhu, P. Johnson, J. Chem. Phys. 94 (1991) 5769.
[19] L. Wang, H. Li, D. Dai, J. Bai, R. Lu, Chin. J. At. Molec. Phys. 14 (1997) 277.
[20] L. Wang, H. Li, C. Ma, J. Bai, R. Lu, Comput. Appl. Chem. 13 (1996) 86.
[21] R.C. Weast, CRC Handbook of Chemistry and Physics, 51st ed., Boca Raton, FL, Chemical Rubber, 1970–1971, p. E-74.
[22] R.S. Freund, High-Rydberg Molecules, in Rydberg States of Atoms and Molecules R.F. Stebbing, F.B. Dunning (Eds.), Cambridge University Press, Cambridge, 1983, p. 355.
[23] F. Merkt, Ann. Rev. Phys. Chem. 48 (1997) 669.
[24] J.A. Schiavone, S.M. Tarr, R.S. Freund, Phys. Rev. A 20 (1979) 71.